Nuclear Engineering and Technology 54 (2022) 4460–4473

Contents lists available at ScienceDirect

Nuclear Engineering and Technology

journal homepage: www.elsevier.com/locate/net

Original Article

Towards grain-scale modelling of the release of radioactive fission gas from oxide fuel. Part II: Coupling SCIANTIX with TRANSURANUS

G. Zullo [a], D. Pizzocri [a], A. Magni [a], P. Van Uffelen [b], A. Schubert [b], L. Luzzi [a, *]

[a] Politecnico di Milano, Department of Energy, Nuclear Engineering Division, Via La Masa 34, 20156, Milano, Italy
[b] European Commission, Joint Research Centre (JRC), Karlsruhe, Germany

ARTICLE INFO

Article history:
Received 24 February 2022
Received in revised form
7 July 2022
Accepted 24 July 2022
Available online 13 August 2022

Keywords:
Oxide nuclear fuel
Radioactive release
Fission gas behaviour
Fuel performance code
TRANSURANUS
SCIANTIX

ABSTRACT

The behaviour of the fission gas plays an important role in the fuel rod performance. In a previous work, we presented a physics-based model describing intra- and inter-granular behaviour of radioactive fission gas. The model was implemented in SCIANTIX, a mesoscale module for fission gas behaviour, and assessed against the CONTACT 1 irradiation experiment. In this work, we present the multi-scale coupling between the TRANSURANUS fuel performance code and SCIANTIX, used as mechanistic module for stable and radioactive fission gas behaviour. We exploit the coupled code version to reproduce two integral irradiation experiments involving standard fuel rod segments in steady-state operation (CONTACT 1) and during successive power transients (HATAC C2). The simulation results demonstrate the predictive capabilities of the code coupling and contribute to the integral validation of the models implemented in SCIANTIX.

1. Introduction

Multi-scale modelling exploits the coupling among different codes or models. In the analysis of a nuclear reactor core, where different physics interact, it represents a methodology to investigate the performance under irradiation of the fuel rods, replacing the use of individual systems (with possible conservative assumptions) for separate (but inter-related) domains with coupled calculations [1,2]. The coupling promotes the transfer of information between systems that describe phenomena occurring at different time and length scales [3,4]. To assess fuel rod safety and performance, conventional fuel performance codes are coupled either with thermal hydraulics, computational fluid dynamics, or neutronic codes [5–7] or with lower-length modules that describe fission product behaviour (e.g., as demonstrated by the coupling between TRANSURANUS and MFPR-F [8]). The current work outlines the multi-scale coupling approach between the 1.5-D integral fuel performance code TRANSURANUS[1] [9,10] and the mesoscale module SCIANTIX [11].

The TRANSURANUS code performs the thermomechanical analysis of the fuel rod by calculating key state variables to describe the fuel and cladding behaviour (i.e., temperature, stress, and strain fields), while SCIANTIX calculates fission gas release and fuel swelling,[2] which impacts the thermomechanical behaviour of the fuel rod. The TRANSURANUS code meets the requirements for a successful coupling with SCIANTIX: high numerical stability and robustness, low computation time, applicability to time scales from milliseconds to years in the same simulation, and suitability for complex scenarios and irradiation experiments. On the other hand, the SCIANTIX code fits the main features of TRANSURANUS: low computational time (i.e., order of milliseconds per call) and consistency of the numerical solutions offered by the solvers, the latter being required to control the numerical error.[3] without compromising its predictive capabilities, as demonstrated within the INSPYRE H2020 project [17–19].

In this work, we describe the coupling between the

* Corresponding author.
E-mail address: lelio.luzzi@polimi.it (L. Luzzi).

[1] For the present work, the v1m6j21 version of the TRANSURANUS code is employed.

[2] SCIANTIX is able to consider the (local) fuel swelling due to fission gas [11] and due to solid fission products in the matrix, within the high burn-up structure (HBS) [12]. In this work, we take into account only the gaseous fuel swelling.

[3] The models implemented in SCIANTIX include non-linearities (e.g., the temperature dependence of parameters for the intra-granular gas and bubble models). Suitable treatment of consequent stiff equations is needed. In SCIANTIX this is ensured by the implemented solver [11,13–15]. Indeed, the consistency of the solvers is verified via the method of manufactured solutions, a rigorous method recommended for the solver verification [16].

https://doi.org/10.1016/j.net.2022.07.018

TRANSURANUS and SCIANTIX and detail the comparison between the stand-alone version of TRANSURANUS and the version coupled with SCIANTIX. Through the coupling, we extend the capabilities of TRANSURANUS (currently relying on the semi-empirical methodology ANS 5.4–2010 [20]) in predicting the amount of radioactive fission gas accumulated in the free volume of the fuel rod, available for release into the primary coolant in the event of a cladding failure. In particular, the present work follows a previous Part I [21], in which we developed a physics-based description of the grain-scale behaviour of radioactive fission gas in UO_2. We implemented the model in SCIANTIX and employed the stand-alone version of the code to reproduce the CONTACT 1 [22,23] irradiation experiment, analysing the release-to-birth ratio of a set of radioactive xenon and krypton isotopes.

The advantages and disadvantages of using physics-based models to describe the behaviour of inter-related phenomena (such as the behaviour of fission gas in oxide materials) are known [24–26]. On one hand, models describing fission gas behaviour offer greater flexibility in their use with respect to empirical correlations, enabling for example their application to normal irradiation, annealing, and transient conditions [27–30]. On the other hand, the computational time to solve physics-based models is longer than that demanded by empirical correlations. Therefore, the numerical implementation of time-dependent models calls for careful consideration [31].

The development of physics-based approaches, able to reproduce the release of radioactive fission products from the fuel rods, is also of interest in current international research programs [32]. Indeed, the evaluation of the radiological consequences of severe accidents is of crucial importance in nuclear safety studies [33,34]. At present, radiological consequence evaluations rely on empirical or semi-empirical methodologies and are based on conservative assumptions [20,35–38]. By updating these methodologies, more realistic evaluations can be produced, improving accident management.

The present work is organized as follows. In Section 2, we describe the coupling between SCIANTIX and TRANSURANUS codes. In Section 3, we describe the CONTACT 1 [22,23] and HATAC C2 [39] integral irradiation experiments and compare them with the calculations of the stand-alone version of TRANSURANUS as well as with those of TRANSURANUS coupled to SCIANTIX (TRANSURANUS//SCIANTIX). Conclusions are drawn in Section 4, and in Appendix A we detail the effect of different models for the coalescence of grain-boundary bubbles on the predicted fission gas release.

2. TRANSURANUS//SCIANTIX coupling

We provide a brief description of the simulation tools applied in the present work, namely, the mesoscale fission gas behaviour module SCIANTIX [11] and the fuel performance code TRANSURANUS [9,10]. Afterwards, we outline the multi-scale coupling approach between the codes.

2.1. SCIANTIX

SCIANTIX is a 0-D open-source computer code designed to reproduce the main phenomena occurring in nuclear fuels (e.g., UO_2 or MOX fuel), at the scale of the fuel microstructure. SCIANTIX is suitable for in-pile stationary and transient, and out-of-pile annealing conditions [19,40,41]. At present, SCIANTIX includes rate-theory models for the description of stable and radioactive fission gas (xenon and krypton) [21,42,43] and helium behaviour [44,45]. In addition, the formation of high burn-up structure is considered [12,46]. For a more detailed description of the SCIANTIX code structure, we refer to Ref. [11]. The code is able to operate both as a stand-alone computer program and coupled to integral thermomechanical fuel performance codes, as long as a suitable code interface is provided [18,47].

2.2. TRANSURANUS

TRANSURANUS is a fuel performance code for the 1.5-D analysis of a single nuclear fuel rod. TRANSURANUS evaluates fuel and cladding state variables (e.g., temperature, stress, and strain fields) during both normal and transient operation, up to accident conditions [9,10]. The code assumes the cylindrical symmetry of the fuel rod so that the thermomechanical analysis is carried out first in a 1-D radial geometry. Afterwards, the computed radial profiles are coupled between adjacent axial slices of the fuel column.

In this work, we focus on the TRANSURANUS output quantities that concern the (stable and radioactive) fission gas behaviour. The current physics-based option for stable fission gas behaviour in TRANSURANUS was developed by Pastore et al. [30]. It describes production, diffusion, precipitation, and release of inert fission gases (xenon and krypton), and couples the release mechanisms to the fuel swelling prediction. Concerning radioactive gas, the semi-empirical ANS 5.4–2010 methodology for evaluating the release-to-birth ratio of short-lived fission gases is adopted [20].

Eventually, thanks to the coupling with SCIANTIX (outlined in the next Section 2.3), TRANSURANUS inherits the SCIANTIX physics-based models for intra- and inter-granular stable fission gas behaviour [12,42,43,48], helium behaviour [44] and radioactive fission gas behaviour [15,21].

2.3. Coupling interface for the TRANSURANUS//SCIANTIX code

SCIANTIX can be selected among the TRANSURANUS input settings as fission gas behaviour module. A coupling interface was needed to ensure the communication between variables common to TRANSURANUS (declared in FORTRAN environment) and SCIANTIX (declared in C++ environment). This communication was set as on *online coupling* between the two codes.[4] The coupling interface has been firstly developed in the framework of the European INSPYRE project [17,18] and finalized in the present work. The interface consists of a set of subroutines built on the FORTRAN 95 BIND attribute [50], declaring the FORTRAN variables as interoperable with the C++ programming language. The subroutine fc_fdef was added to TRANSURANUS and in parallel SCIANTIX was endowed with a module (fc_api) that implements the same functions defined in the fc_fdef subroutine.

The coupling strategy implies the call of SCIANTIX at each mesh point, time-step, and convergence iteration of the TRANSURANUS code (namely, at level 3 of the TRANSURANUS code structure [10]). SCIANTIX receives from TRANSURANUS local quantities (fuel temperature, fission rate density, hydrostatic stress, grain radius) and the time step size. At each discretized radial position of the considered axial slice of the fuel column, SCIANTIX calculates the local gaseous swelling[5] and fission gas release. Then, these quantities are transferred back to TRANSURANUS and affect the overall thermomechanical behaviour of the fuel rod [47].

Besides, as part of this work, the coupling interface was upgraded to extend the TRANSURANUS restart option with the SCIANTIX

[4] *Online coupling* is used in reference to a transfer of data across different systems that occurs directly within the computer memory, during program execution. It is accomplished through the coupling interface and is opposed to the *offline coupling* method, which involves an exchange of information through input/output files between two systems [49].

[5] The models implemented in SCIANTIX allows the calculation of intra-granular gaseous swelling (i.e., due to intra-granular bubbles) and inter-granular gaseous swelling (i.e., due to grain boundary bubbles) [11,30].

variables. This action has required to extend the TRANSURANUS arrays containing the SCIANTIX information (i.e., r8_comp and r4vek), stored in 100% densely packed form in memory [51]. The TRANSURANUS code allows the users to select a restart option, to append to a basic run one (or more) additional run(s) accounting for fuel rod re-fabrication phases, e.g., when the composition of the fill gas is modified. The transfer of data between two successive simulations (the basic run and the restart run) happens by means of the generation of a binary file containing the values of all the variables of the code at a determined (user-defined) time instant. Changing TRANSURANUS models options and/or parameters between successive simulations can be done in two equivalent ways. Both require a specific external program (restart module), to be built by the user as a dedicated FORTRAN 95 routine. The user can then either compile the restart routine and build it together with the other routines of TRANSURANUS to generate one executable, or generate a separate executable referred to as the restart module. The user can select which way to modify the TRANSURANUS variables stored in the binary file via a dedicated input option. The corresponding changes made to the interface lead to the correct (and automatic) placement of SCIANTIX variables within the restart binary file, to properly preserve the reading and writing phase in TRANSURANUS. The upgrade of the coupling interface to include the restart option in the coupled version of the code was necessary for the present work, as this option is required for the correct simulation of irradiation experiments with re-fabricated fuel rods segments (as for the CONTACT 1 [22,23] and HATAC C2 [39] irradiation experiments, considered in Section 3). In addition, it paves the way for future extensions of the code validation database to fuel rod simulation in accident conditions (e.g., the experiments undertaken within the Fuel Modelling in Accident Conditions (FUMAC) research project [52]).

3. Code assessment against integral irradiation experiments

The TRANSURANUS fuel performance code [9,10], coupled with the fission gas behaviour module SCIANTIX [11], is employed to test at the rod scale the impact of the physics-based models that describe the fission gas evolution in the UO_2 fuel grains [11,21,42,48].

To assess the new coupled code capabilities in reproducing both stable and radioactive fission gas release, we consider two representative irradiation experiments from the IFPE database, CONTACT 1 [22,23] and HATAC C2 [39]. CONTACT 1 was focused on the fuel rod behaviour irradiated in stationary conditions. HATAC C2 investigated the fuel behaviour during a sequence of power transients. The figures of merit for the assessment against CONTACT 1 are the fractional release of stable fission gas and the release-to-birth ratio of short-lived fission gases [22,23]. The comparative analysis is supported by applying the ANS 5.4–2010 semi-empirical methodology [20] to evaluate the release-to-birth ratio of short-lived fission gas. The assessment against the HATAC C2 experiment is performed by comparing the fractional release of stable fission gas and the release rate of the short-lived ^{133}Xe [39].

3.1. Description of the CONTACT 1 experiment

The CONTACT 1 experiment is detailed in Refs. [22,23]. We focus on the CONTACT 1 - FRAMATOME fuel sample, a short (7 cm) column of five UO_2 pellets wrapped in their original Zr-4 cladding. The irradiation phase took place at the Siloe nuclear reactor [53]. The fuel column was thermally insulated and placed in a pressurized (13 MPa) loop to best represent the cladding creep-down rate of a pressurized water reactor (PWR). The nucleate boiling regime provided an external cladding temperature of about 330 °C. The

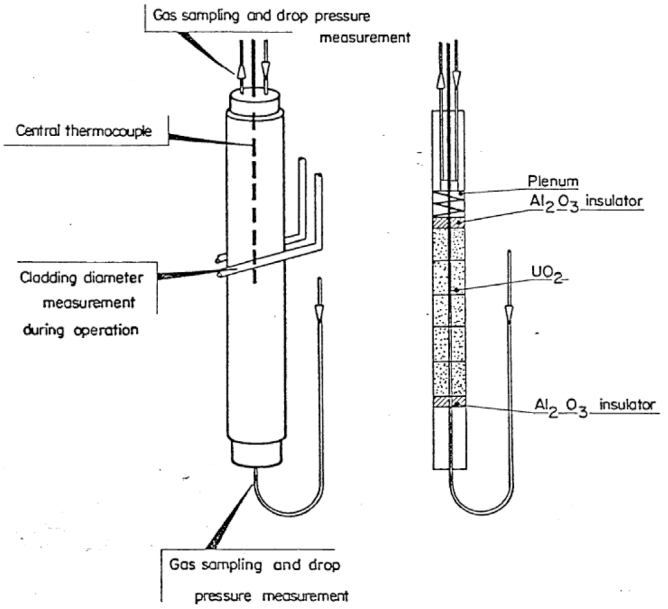

Fig. 1. Scheme of the setup employed during the CONTACT 1 test [22].

fuel sample was irradiated at a constant linear rating close to 40 kW m^{-1}, with negligible axial power variations, i.e., less than 2% [22]. We show a scheme of the experimental setup in Fig. 1. The fuel rod was equipped with a thermocouple placed at the mid-plan of the fuel pellet stack to measure the centerline temperature, two fingers to measure the cladding outside diameter at a fixed axial position, a differential gauge to measure the pressure drop through the fuel rod by imposing a helium flow and a helium sweeping device to collect gaseous fission products.

The CONTACT 1 experiment began in September 1978 and ended in July 1980 and each irradiation cycle consisted of 21–24 days of irradiation per month. The experiment got interrupted from April to September 1979 due to an accidental introduction of air into the water loop. After this event, a diameter increase of 60 μm was measured. Moreover, in September 1979 the composition of the filling gas has been changed from 1 MPa of He to 0.1 MPa of Ne and the irradiation continued up to approximately 22 MWd kgU^{-1}. We consider the detected oxide layer (together with its contribution to the thermal resistance of the fuel-cladding system) and the change in gas composition by applying the TRANSURANUS restart option after the reactor shutdown. We collected the details of the irradiated rods in Table 1.

The results of the CONTACT 1 test regard measurements of the fuel centerline temperature (FCT) (see Fig. 3), the fractional fission gas release (FGR) through the ^{85}Kr (Fig. 4), and the release-to-birth ratio (R/B) of short-lived fission gases, with half-live between 5.29 days (^{133}Xe) and 3.18 min (^{89}Kr). We reproduce the CONTACT 1 experiment using the TRANSURANUS mechanistic fission gas behaviour model with its standard parameters [9,10,30] and the TRANSURANUS//SCIANTIX coupled-code version, which relies on the SCIANTIX [11] fission gas behaviour description[6] with its default model parameters for the stable and radioactive fission gas

[6] At the inter-granular level, both models consider a mechanistic description of the grain-boundary bubble growth, coalescence, and interconnection (that determine the grain-boundary swelling and fission gas release) but differ in the adopted coalescence model. In addition, SCIANTIX includes a physics-based model for the evolution of the intra-granular fission gas bubbles coupled to the aforementioned grain-boundary model, which also affects the fission gas release and swelling prediction [42].

Table 1
Specifications of the fuel rod used in the CONTACT 1 (C 1) experiment [22].

	Parameter	u.o.m.	C 1
Pellets	Length	mm	14
	Diameter	mm	8.19
	Dish depth	mm	0.13
	Dish radius	mm	14.73
Cladding	Internal diameter	mm	8.36
Cladding	External diameter	mm	9.50
Plenum	Length	mm	7.7
Int. pressure		MPa	1
Fuel column	Number of pellets		5
	Enrichment	%	4.95
	Geometric density	% TD	95
Irradiation	Nominal rating	kWm^{-1}	40.5
	Peak rating	kWm^{-1}	41
	Average rating	kWm^{-1}	36
	Fast flux ($E > 1$ MeV)	$m^{-2}\ s^{-1}$	6.50×10^{17}
	Discharge burn-up	MWd kgU^{-1}	22
	Clad ext. temperature	°C	330
System pressure		MPa	13

behaviour [11,21].

3.2. Simulation results

Fig. 2 shows the power history used as input for the TRANSURANUS calculation. Fig. 3 shows the FCT from TRANSURANUS and TRANSURANUS//SCIANTIX calculations, along with measurements obtained during the experiment. The impact of SCIANTIX in the TRANSURANUS temperature calculation is minimal. This result was expected since TRANSURANUS is able to analyse experiments with "open" rods such as the CONTACT 1, characterised by a gas sweeping system that constantly removes the released fission gas, minimizing the consequence on the gap conductance. With respect to the TRANSURANUS stand-alone code, the coupling with SCIANTIX yields a lower FCT before 8 MWd kgU^{-1}, and a higher FCT afterwards. Since we attribute this behaviour primarily to the predicted fission gas release (Fig. 4), we elaborate on it in what follows and in Appendix A. The measured FCT shows a decrease of about 80 °C, from the beginning of the experiment up to about 7 MWd kgU^{-1}, that is when the experimental reports infer the gap closure. Both codes capture the decrease in temperature over the same burn-up range. After the reactor shutdown, the FCT reading remains nearly constant around 1450 °C while the codes overestimate it by about 50 °C. The difference with the experimental data (within the 5%) is attributed to the reconstructed power history fluctuations combined with measurement instrumentation oscillations.

Fig. 4 shows the measured fractional fission gas release (measured at specific points in time and connected by means of lines) against the calculations of the two codes. With respect to the experimental points, both codes overestimate the fission gas release throughout the irradiation, albeit within the commonly accepted uncertainty band, that is a factor of two [54]. The overestimation of the fission gas is coherent with the higher predicted fuel temperature (Fig. 3), because of the feedback of the gas on the gap conductance and on the fuel temperature. The calculations of the two codes differ due to the different models adopted to describe the behaviour of the fission gas. The TRANSURANUS code remains closer to the experimental points, while the coupled code predicts a higher fission gas release, with an error on the final value of almost 30%. We ascribe this difference to the different treatment of the grain-boundary coalescence model, that influences the accumulation of the gas on the grain boundary and the subsequent release. Considering a single fuel grain, with N representing the density of grain-boundary bubbles and A their projected area on the grain boundary, the mechanistic TRANSURANUS model considers a coalescence rate of $\frac{dN}{dA} = -\frac{6N^2}{3+4NA}$ based on the work of Pastore et al. [30], while SCIANTIX adopts the White equation $\frac{dN}{dA} = -2N^2$ [55]. The coalescence rate proposed by White leads to a faster description of the process (since the product NA achieves a maximum value near 0.5 [48,55]) and also to increased coverage of the grain-boundary surface with bubbles (i.e., an increased bubble interconnection). For this reason, as the irradiation proceeds, the fission gas release predicted by SCIANTIX is higher than the TRANSURANUS prediction (Fig. 4). In Appendix A, we detail an example to highlight the inter-granular gas dynamics.

The computed fission gas release encompasses two separate contributions: the diffusional release given by grain-boundary bubble growth and coalescence, and the burst release attributed to micro-cracking of the grain boundaries due to sudden temperature variations. The latter effect is included in SCIANTIX with a semi-empirical description of the reduction in gas storage capacity at the grain boundaries [48]. The release of fission gas from the burst model is essential for proper simulation in the cases under

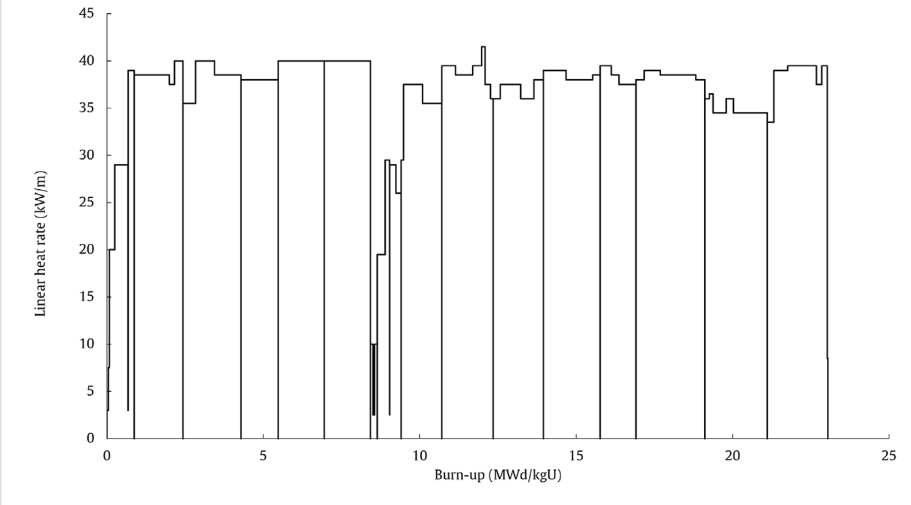

Fig. 2. CONTACT 1: Linear heat rate used as input for the TRANSURANUS calculation.

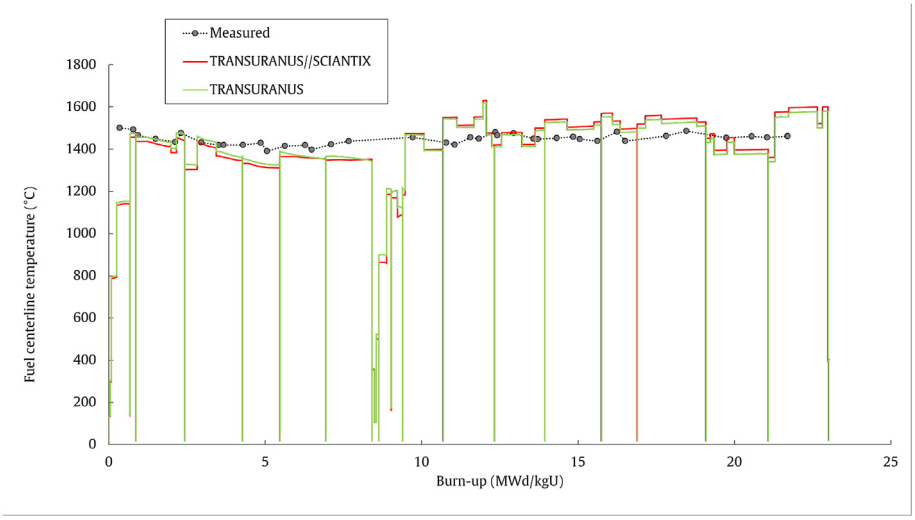

Fig. 3. CONTACT 1: comparison of the measured fuel centerline temperature (grey dots) with the predictions of TRANSURANUS (green line) and TRANSURANUS//SCIANTIX (red line). (For interpretation of the references to colour in this figure legend, the reader is referred to the Web version of this article.)

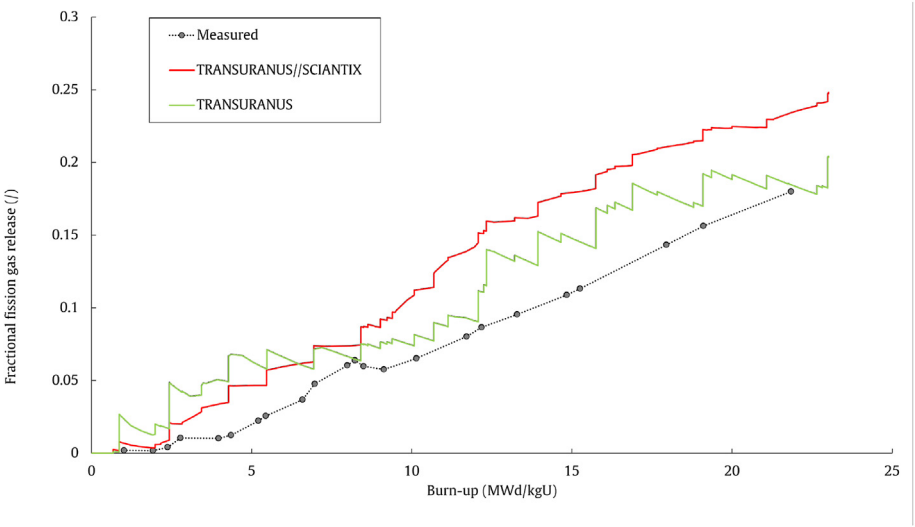

Fig. 4. CONTACT 1: comparison of the measured fractional fission gas release (FGR) (grey dots) with the predicted FGR by the mechanistic TRANSURANUS option for the fission gas behaviour [30] (green line) and by the coupled code TRANSURANUS//SCIANTIX (red line) [11]. (For interpretation of the references to colour in this figure legend, the reader is referred to the Web version of this article.)

consideration, as the gas contribution from grain-face separation due to micro-cracking represents a significant contribution to the released gas. However, the semi-empirical nature of the model implies some limitations in its applicability, contributing to an overestimation of the fission gas release that could be reduced by improving the model parameters.[7]

Lastly, we consider the release-to-birth ratio (R/B) of the short-lived ^{85m}Kr and ^{133}Xe, for radioactive fission product release. For comparative analysis, we provide the results of the ANS 5.4–2010 methodology, a state-of-the-art semi-empirical approach to estimate the R/B in stationary conditions according to the thermal power generated per unit length of the fuel rod and the burn-up. The methodology is described in detail in the background report [20] and in Part I of this work.[8] Also, we show the R/B curves computed with the SCIANTIX stand-alone version, obtained in Part I with a 0D representation of the CONTACT 1 experiment [21].

[7] The model for the grain-boundary micro-cracking is strongly sensitive to the inflection temperature T_{infl}, as demonstrated in Ref. [48]. The inflection temperature is defined as $T_{infl} = \alpha + \beta \exp(-bu/\gamma)$, where bu is the burn-up and α, β, γ are coefficients derived from a best-estimate fit of experimental data. A first improvement of the mentioned model could start from a modification/redefinition of the inflection temperature, preserving the applicability of the model in the code.

[8] In Part I we detailed the SCIANTIX modelling for the radioactive fission gases at the intra- and inter-granular scale of the fuel grain. The intra-granular radioactive gas behaviour is built on the time-dependent solution of the diffusion-decay equation in an equivalent spherical grain [15,56,57]. The trapping in and re-solution from intra-granular gas bubbles are approached in accordance to Refs. [27,58,59]. The inter-granular radioactive fission gas behaviour follows the legacy approach for the stable fission gas accumulation on the grain-boundary bubbles [11,30,55,60], extended by considering the loss of the isotopes due to the decay process [21].

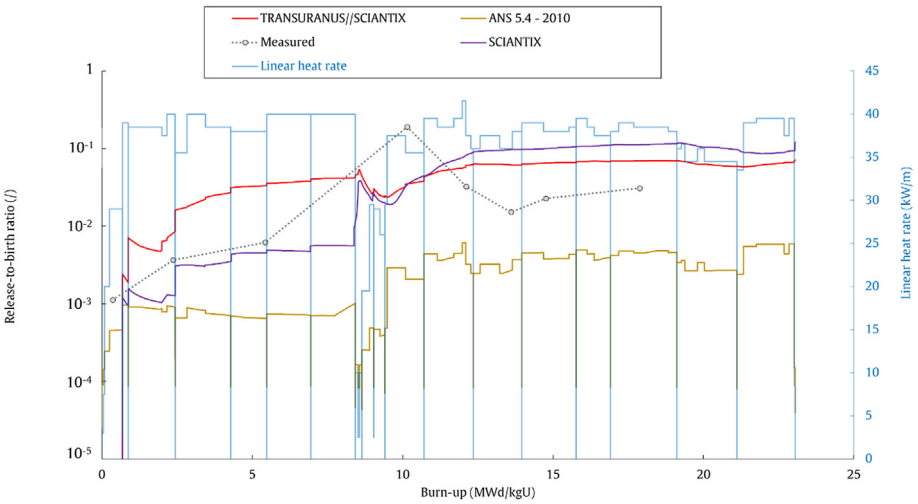

Fig. 5. CONTACT 1: comparison of the ^{133}Xe measured release-to-birth ratio (grey dots) with the release-to-birth ratio predicted by the ANS 5.4–2010 methodology [20] (gold solid line), the stand-alone version of the SCIANTIX code [11] (purple solid line) and TRANSURANUS//SCIANTIX (red solid line), as a function of the fuel rod burn-up. Also, the input linear heat rate is included on the secondary axis (blue line). (For interpretation of the references to colour in this figure legend, the reader is referred to the Web version of this article.)

From Figs. 5 and 6, we discuss the behaviour of the release-to-birth ratio of the short-lived isotopes ^{133}Xe and ^{85m}Kr.[9] The R/B dynamics predicted by TRANSURANUS//SCIANTIX are closer to the expected physical behaviour. This is a consequence of the model implemented in SCIANTIX, describing the peculiar phenomena of production, (intra-granular) diffusion and decay as inter-related and mutually interactive [21]. The approach to an asymptotic value (more evident after 12 MWd kgU^{-1} in Figs. 6 and 5) results from the competition among production, diffusion and radioactive decay. This prediction differs from the one given by the semi-empirical ANS 5.4–2010 methodology, based on the equilibrium solution of the diffusion-decay equation. In particular, the ANS 5.4–2010 methodology is not designed to describe the time evolution of radioactive fission gas as a consequence of the physical phenomena of intra-granular diffusion, grain-boundary accumulation and release due to bubble interconnection. Rather, it aims to produce a conservative estimation of R/B as a function of local values of fuel temperature and linear heat rate.

The R/B calculated with the SCIANTIX stand-alone code were obtained from a representative lumped simulation of the experiment.[10] The fact that we are analysing the experiment with a fuel performance code that calls the SCIANTIX module at each radial and axial node allows us to point out that the increase in the R/B curves near 8 MWd kgU^{-1}, predicted by the lumped simulation in Figs. 5 and 6, is related to the diffusional release of the gas accumulated in grain-boundary bubbles.[11] The diffusional release does not occur in a clear-cut manner in the coupled version of the code because it is controlled by the fuel temperature value (a higher temperature promotes the intra-granular diffusion of gas towards the grain-boundary bubbles, the gas accumulation increases the bubble coalescence and the subsequent release) and the contribution of gas that is released from the internal (hotter) fuel region exceeds the contribution that is due to the burst release ascribed to micro-cracking.

3.3. Description of the HATAC C2 irradiation experiment

The specifications of the HATAC C2 mother rod are summarized in Table 2. The HATAC C2 irradiation experiment consisted of an initial base irradiation of a PWR fuel rod with UO_2, in the Fessenheim-1 Nuclear Power Plant [39] up to an average burn-up of 45.79 MWd kgU^{-1} (after four annual irradiation cycles). The nominal average linear power in the core was 17.48 kW m^{-1} while the maximum linear heat rate was 22.5 kW m^{-1}. Fig. 7 details the linear heat rate evolution provided as input for the TRANSURANUS simulation. The inlet and outlet temperatures of the coolant were 284 °C and 323 °C, respectively, with a coolant pressure of 15.5 MPa. The initial enrichment of the UO_2 fuel was 3.2% ^{235}U. The mother rod was filled at room temperature with helium at 34.5 bar. Experimental analysis of the mother fuel rod indicated a low release of (stable) fission gas from athermal mechanisms, while most of the fission gas (> 99.5%) was retained within the fuel.

After the base irradiation, a section was cut from the mother rod and the short fuel rod segment was re-irradiated in the Siloe research reactor [39,53] for eight monthly cycles (from April 1989 to May 1990). The re-irradiation period included a sequence of short power transients (see Fig. 8), to reproduce the expected power variations in load follow or frequency control mode. The first five power transients were run at a linear heat rate between 18 and

[9] As stated in the IFPE documentation of the CONTACT programme [22,23] and in Part I of this work [21], the measurement of ^{133}Xe at 10 MWd kgU^{-1} visible in Fig. 5 shows a significant increase at 10 MWd/kgU^{-1}. The documentation exhibits a lack of information about the experimental uncertainty of the measurements, but the ^{133}Xe is known to be subjected to larger uncertainty in comparison with that on other isotopes (e.g., ^{85m}Kr) [20]. It is reasonable to ascribe the aforementioned ^{133}Xe release-to-birth ratio increase to instrumentation errors because it is not reflected in the other release curves [21–23]. Furthermore, the linear connection between the points measured at successive time points should not be confused with real release evolution points.

[10] SCIANTIX being a grain-scale code, it works with local quantities (fuel temperature, fission rate density and hydrostatic stress of the fuel). The results obtained from the stand-alone simulation of SCIANTIX, shown in Figs. 5 and 6, were calculated on the basis of a lumped simulation of the CONTACT 1 experiment, performed with the TRANSURANUS stand-alone code, in which the aforementioned quantities were radially averaged. The procedure and the results obtained are described in detail in Part I of this work [21].

[11] Specifically, the release of gas from grain-boundary bubbles is described through the concept of fractional coverage (the total bubble area per unit grain boundary area). When the threshold value for the fractional coverage is reached, a fraction of gas stored in the grain-boundary bubbles is released. This model (based on Refs. [30,55,60]) is implemented in TRANSURANUS and considered within the SCIANTIX mechanistic description of fission gas behaviour.

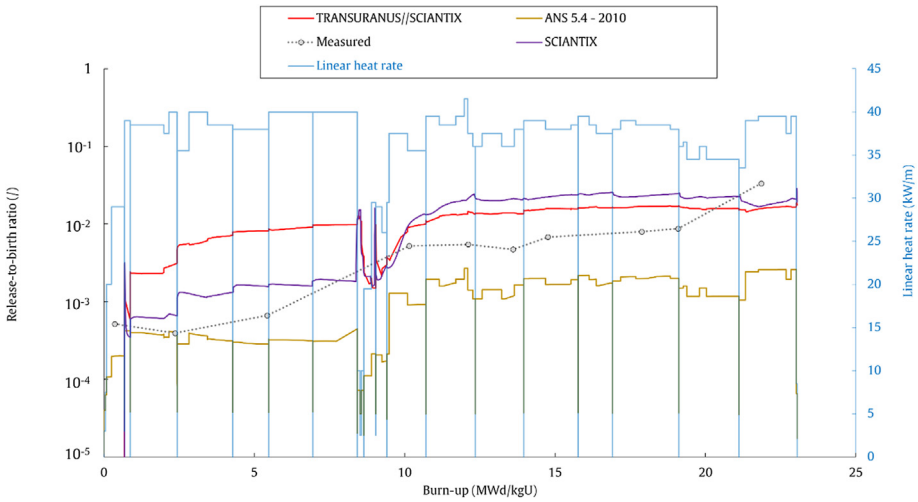

Fig. 6. CONTACT 1: comparison of the ^{85m}Kr measured release-to-birth ratio (grey dots) with the release-to-birth ratio predicted by the ANS 5.4–2010 methodology [20] (gold solid line), the stand-alone version of the SCIANTIX code [11] (purple solid line) and TRANSURANUS//SCIANTIX (red solid line), as a function of the fuel rod burn-up. Also, the input linear heat rate is included on the secondary axis (blue line). (For interpretation of the references to colour in this figure legend, the reader is referred to the Web version of this article.)

Table 2
HATAC mother rods characteristics [39].

Parameter	HATAC C2
Fuel rod	
Initial diametrical gap size (mm)	0.191
Fuel stack length (m)	3.6594
Pellet number	260
Total gap volume (cm^3)	15.2
Filling gas	He
Initial gas pressure (bar)	34.5
Plenum length (cm)	15.77
Cladding	
Alloy	SRA Zircaloy
Outer diameter (cm)	0.9524
Inner diameter (cm)	0.8384
Fuel pellets	
Fuel	UO_2
^{235}U enrichment (%)	3.138
Pellet outer diameter (cm)	0.8193
Pellet length (cm)	1.401
Dishing number per pellet	2
Dish hemispheric radius (cm)	1.473
Dish depth (cm)	0.0305
Relative density (% TD)	93.984
Volume density (g cm^{-3})	10.301
Average grain size (μm)	7.05 to 7.99
Open porosity (%)	0.1
End plugs	Zyr4
Spring	
Material	Steel AISI 302
Wire diameter (cm)	0.1705
Spire diameter (cm)	0.815
Number of spires	45

28 kW $^{-1}$ while the last five were run between 20 and 29 kW $^{-1}$. The high power holding times lasted approximately 3 h, and the power ramp rate to reach these peaks was 5 kW m^{-1} min^{-1}.

The HATAC experimental programme was aimed at analysing the mechanisms of fission gas release at fuel burn-up above 35 MWd kgU^{-1} and during power cycling operations[12] [39]. The instrumentation used to measure the gas release during the re-irradiation period consisted of a sweeping device for online measurement of fission gases (both stable and radioactive isotopes), similar to what was done in the CONTACT 1 experiment.

3.4. Simulation results

We simulate the base irradiation conducted in the Fessenheim-1 unit and the subsequent re-irradiation in the Siloe reactor with the TRANSURANUS code, used both in its stand-alone version and coupled to SCIANTIX. The transition between the two different irradiation configurations is performed through the use of the restart option, which is possible thanks to the updated interface between the two codes.

Fig. 9 illustrates the measurement of the fractional FGR against the code calculations. A significant contribution to the measured gas release comes from the initial power (and thus temperature) variation, accounting for about 4% of the total FGR inventory. The formation of micro-cracks can induce a sudden release of gas from closed bubbles, which are opened by the cracks formed.

During each transient, the temperature rise provokes an increase in the gas diffusivity, causing the fuel grains to release the gas accumulated in or close to the interconnected grain boundaries. The sweeping helium stream was supposed to flow along the fuel stack. When decreasing the power, the temperature decreases as well and the fission gas release is slowed down. The gas release measured during power reductions is attributable to the amount of gas that is produced and accumulated during preceding stationary power phases. This amount of gas remains either trapped in cracks, closed porosity (e.g., the network of grain-boundary bubbles), void volumes or in the closed gap when the fuel expands at high temperature. Then, during power reductions, the opening of the gap and fuel cracks provides a path for the gas to be released [48,61].

The FGR predicted by the TRANSURANUS mechanistic settings (Fig. 9) tends to underestimate the data. On the other hand, using SCIANTIX with the micro-cracking model activated yields a better agreement with the experimental data. With respect to the SCIANTIX predictions, it is presumed that the TRANSURANUS underestimation is mainly a consequence of the different treatment of

[12] The HATAC programme encompassed two similar experiments, HATAC C1 and C2, characterised by an average burn-up of 33.34 kgU^{-1} and 45.79 kgU^{-1}, respectively. Owing to the increased availability and quality of measured experimental data, as well as the more interesting burn-up range, we deemed it appropriate to deal with the HATAC C2 case first.

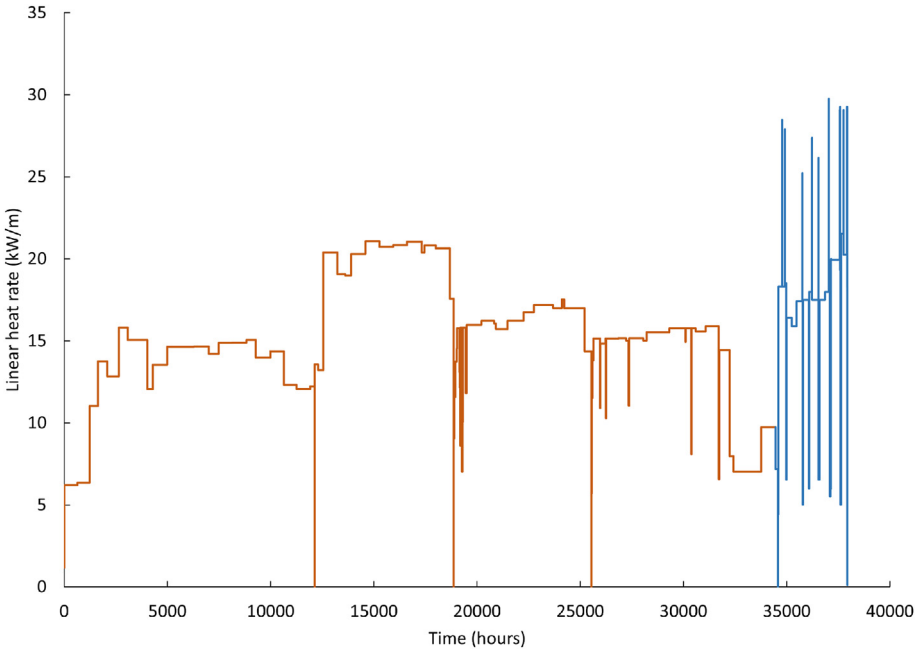

Fig. 7. HATAC C2: In orange, the linear heat rate during the base irradiation (in Fessenheim-1), and in blue the re-irradiation phase (in Siloe), used as input for the TRANSURANUS calculations. (For interpretation of the references to colour in this figure legend, the reader is referred to the Web version of this article.)

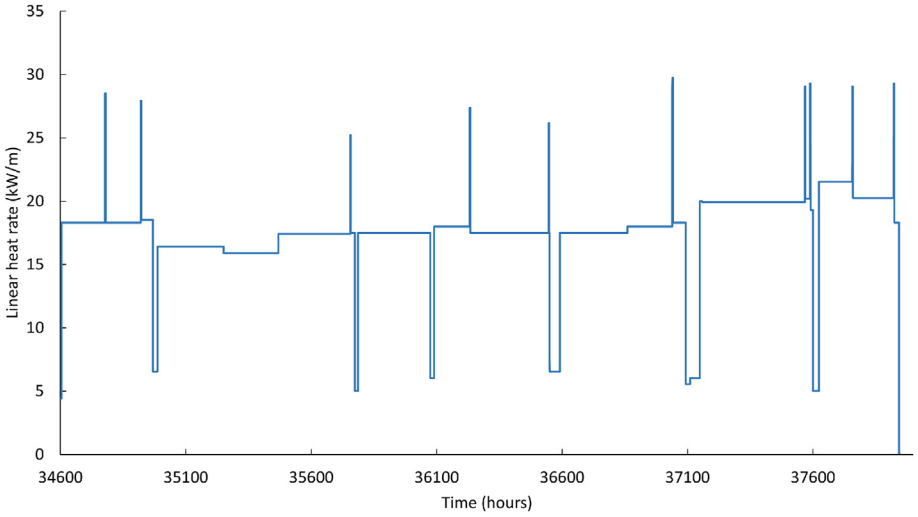

Fig. 8. HATAC C2: Enlargement of Fig. 7, detailing the re-irradiation phase (in Siloe) and the sequence of ten successive power transients.

gas at the grain-boundary bubbles, as we explained in Section 3.2 and detail in Appendix A. In particular, the discrepancy between the two codes can be explained by considering that, according to TRANSURANUS, the grain-boundary bubbles retain more gas and this results in a lower release than that predicted by SCIANTIX. (Fig. 4). Identifying the most effective mechanistic modelling to describe the release of fission gas is not a straightforward task and is beyond the scope of this article. The current paper intends to illustrate that the coupling of SCIANTIX to the fuel performance code provides results that show qualitative agreement with the experimental data (in terms of absolute values and dynamics), within the classical uncertainty ranges that exist for FGR calculations [54].

The use of SCIANTIX without the micro-cracking model activated, results in a lower FGR prediction, as expected from the absence of this contribution to the release. In the HATAC C2 test, the micro-cracking model appears to be central in the correct evaluation of the release, as the experiment is designed to investigate rapid power variations.

The use of the SCIANTIX module enables TRANSURANUS to evaluate the time-dependent release of short-lived fission gases, as a consequence of the development undertaken in the previous work [21], describing the radioactive gas behaviour. Fig. 10 shows the predictions of the ^{133}Xe release rate measured during each transient, from the 3rd to the 10th. A general summary of the release rate pattern observed in the analysed transients can be

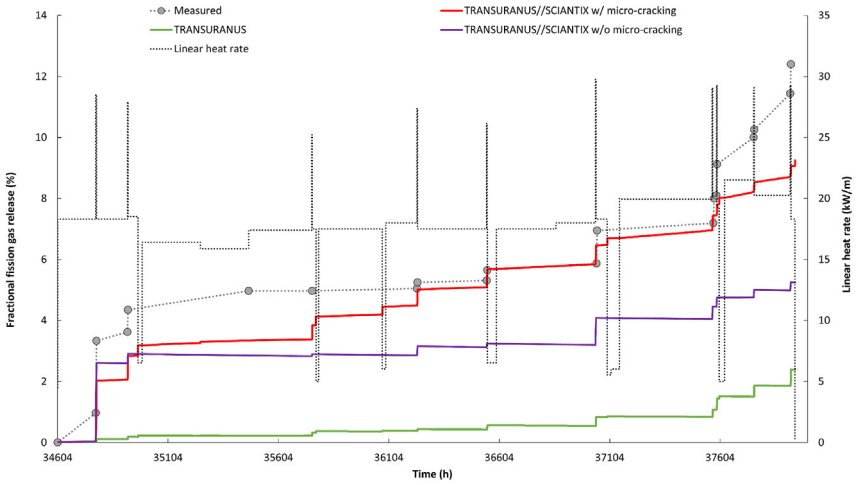

Fig. 9. HATAC C2: Stable fission gas release measured during the re-irradiation phase (grey dots) compared to mechanistic TRANSURANUS (green line) calculations, the TRANSURANUS//SCIANTIX calculations with the micro-cracking model (red line) and without the micro-cracking model (purple line). The linear heat rate is also reported (blue dotted line). (For interpretation of the references to colour in this figure legend, the reader is referred to the Web version of this article.)

proposed as follows:

- During power increases, the ^{133}Xe accumulated at the grain-boundary is vented out from the fuel. This corresponds to the first increase in the measured release rate.[13]
- During intermediate phases at constant power, the ^{133}Xe diffusion-decay process tends towards the equilibrium and the rate tends to a constant value.
- During power decreases, the associated stress variations lead to the gas venting from the fuel and a concomitant spike in the measured release rate.

Among the various sources of uncertainty, for example due to experimental accuracy needed to detect the short-lived ^{133}Xe [20], or due to our simplified grain-boundary modelling, we discuss the model for gas release due to micro-cracking. In fact, having a semi-empirical nature, its applicability to this specific power cycling experiment may alter the release rate kinetics. In Fig. 10 we compare the experimental data[14] with the calculated release rates, both with and without the effect of the burst release due to micro-cracking.

It is noted that the behaviour of the computed release rates is generally closer to the behaviour measured during the power increase and the successive constant power holding, rather than during the power decrease. Because the release rate evolution is qualitatively unaffected by the inclusion of the burst release due to micro-cracking (during the power increases and constant power holding), it is reasonable to assume that the release dynamics is controlled by the diffusional release model. On the contrary, during the power decrease, it is evident that the burst release due to micro-cracking produces an overestimation of the release rate (i.e., of one order of magnitude on the value of the release rate). Although in this case the diffusional contribution alone produces an overestimation of the data, it appears that forthcoming developments of the micro-cracking effects are possible and should consider the asymmetric representation of the release during power increases and decreases.

Another source of model-related uncertainty, which can affect the calculations, concerns the description of grain-face, grain-edge, and grain-corner porosity [27,55] in SCIANTIX. As a qualitative assessment, it is possible that the high release rate measured during the first power increase may lead to a sudden emptying of the grain edge porosity, resulting in depressurization and collapse mechanism of the interconnected porosity. This mechanism would in turn cause a lower experimental release rate measured at the depressurization stage [27,62–64]. Nevertheless, a complete description of the grain-boundary porosity is a complex task that calls for the use of empirical parameters and assumptions affected by uncertainty and a follow-up in this direction would require more supporting experimental data to rely on.

4. Conclusions

In the present work, we first outlined the extended coupling approach between the TRANSURANUS fuel performance code and the mesoscale fission gas behaviour module SCIANTIX. Subsequently, we illustrated the coupled version of the code by simulating two different types of irradiation experiments. The CONTACT 1 case is representative of stationary irradiation conditions of a UO_2 rodlet, while the HATAC C2 case is representative of power cycling.

For both cases, the results obtained with the coupled codes are encouraging. Compared to the original coupling interface that was implemented, the most relevant update concerns the integration of the restart capability (specific of TRANSURANUS), which allowed comparison with the experiments considered and paves the way for the extension of the SCIANTIX validation database (e.g., with tests representing LOCA conditions).

Through this improvement, the inclusion of the models for stable fission gas behaviour allows TRANSURANUS to fully complement its mechanistic model with an interesting alternative, based on a new code which benefits from substantial developments in the field of fission gas modelling and, above all, has an open-source licence. This last aspect also makes SCIANTIX an option for various integral performance codes (e.g., BISON, GERMINAL, OFFBEAT, FRAPCON, FRAPTRAN). With regard to radioactive gas, the

[13] Only in Fig. 10g the initial spike is not present, in the measurement of the 9th transient. Because of the lack of any explanation in the documentation of the experiment, we assume that the measurement point was not taken during the power increase.

[14] In the IFPE documentation, it is indicated that the released fission gas was collected from the helium stream, dispatched to an analysis laboratory, and measured with a Ge–Li detector. The data sets for fission gas release fraction and release rates were then derived from a computer program. Therefore, the reported experimental measurements were not instantaneous but processed *a posteriori*, and thus may suffer from an additional contribution of uncertainty, which however was not quantified.

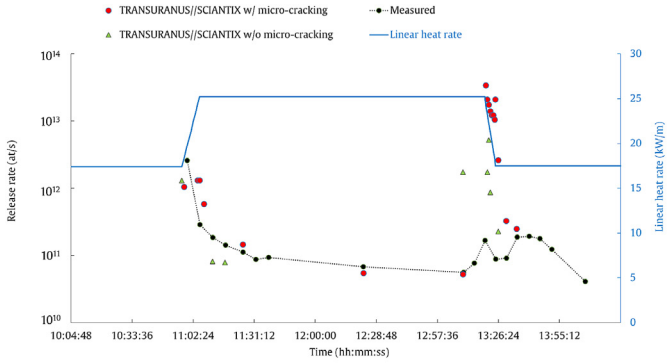

(a) HATAC C2 – 3rd transient.

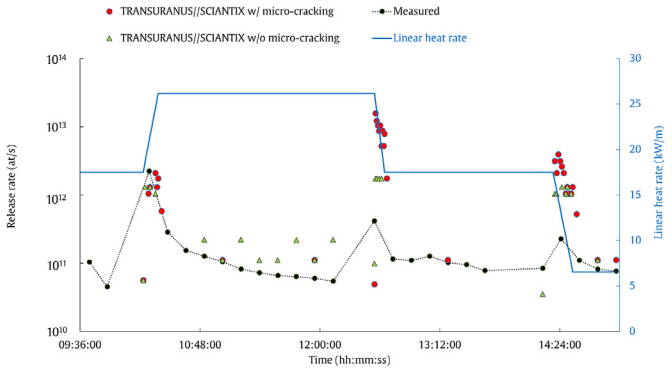

(c) HATAC C2 - 5th transient.

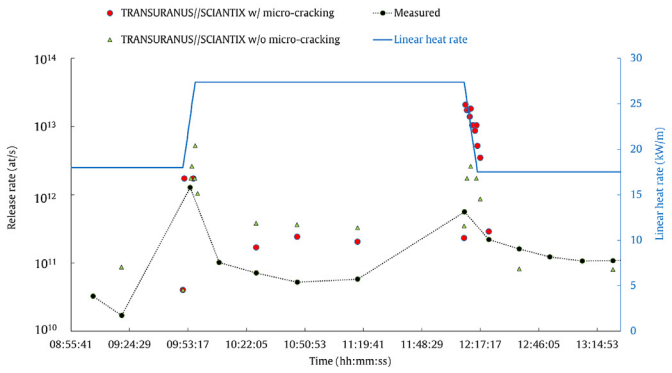

(b) HATAC C2 - 4th transient.

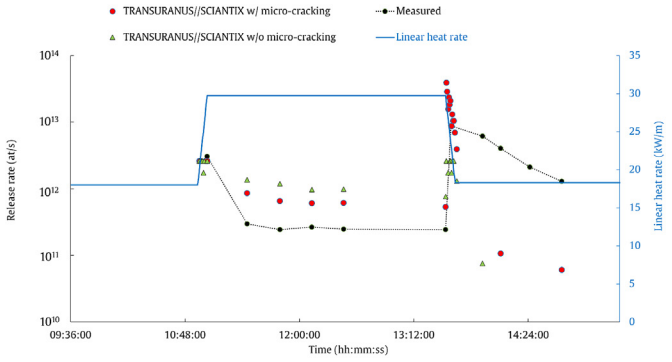

(d) HATAC C2 - 6th transient.

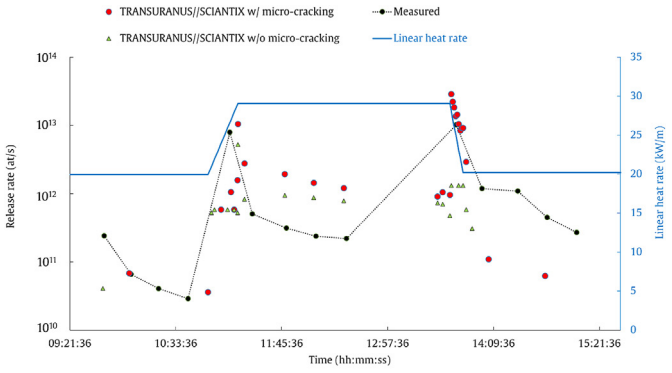

(e) HATAC C2 – 7th transient.

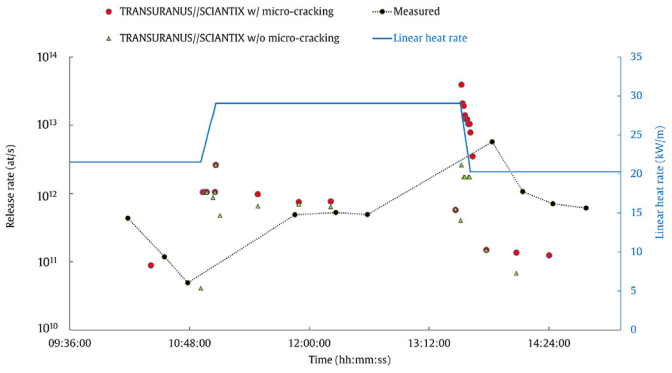

(g) HATAC C2 – 9th transient.

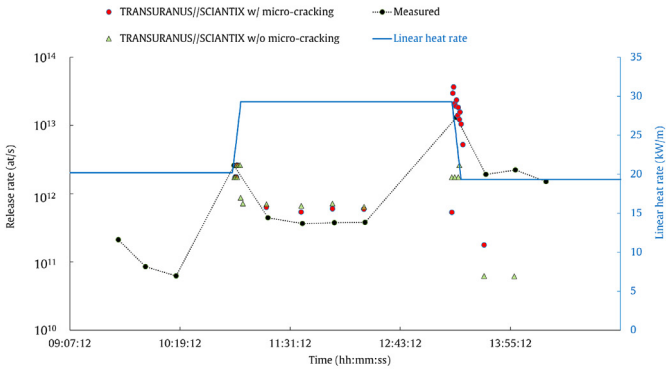

(f) HATAC C2 - 8th transient.

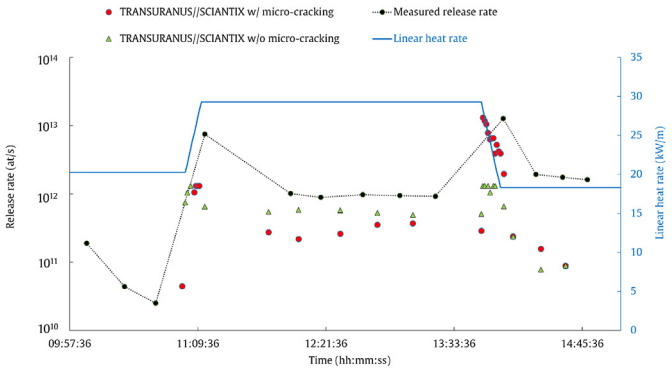

(h) HATAC C2 - 10th transient.

Fig. 10. HATAC C2 – Showcase of the ^{133}Xe release rate measured during the considered power transients. The measurements (black dots) are compared against the TRANSURANUS//SCIANTIX calculation considering the burst release contribution from the micro-cracking (red dots) and neglecting it (green triangles). (For interpretation of the references to colour in this figure legend, the reader is referred to the Web version of this article.)

analysis presented in this paper showed that SCIANTIX enables TRANSURANUS to reproduce the dynamics of release and its evolution during irradiation. This aspect constitutes a milestone for modelling radioactive gas without calibration of specific parameters as in the ANS 5.4–2010 methodology, under both constant and transient conditions. Moreover, the prediction of the radioactive release in terms of release-to-birth ratio is more adherent to the expected variations during irradiation, while the ANS 5.4–2010 is driven solely by the imposed linear heat rate. Nevertheless, the calculated release rates of the short-lived ^{133}Xe isotope require further attention, also considering the large uncertainties pertaining to ^{133}Xe measurements. They reveal only a partial agreement with the measurements, the error reaching even an error of an order of magnitude. From a preliminary analysis, of the model for burst release due to grain-boundary micro-cracking, we could identify the need to revise this model. However, a more detailed and more elaborate analysis is necessary to draw definite conclusions.

Lastly, from the analysis of the results of the two complementary cases analysed in this paper, the potential of the coupled version of TRANSURANUS with SCIANTIX could be highlighted. The availability of coupled codes can be relevant for their application in different European Countries where the evaluation of radioactive elements is part of the licensing procedure.

Declaration of competing interest

The authors declare that they have no known competing financial interests or personal relationships that could have appeared to influence the work reported in this paper.

Acknowledgements

The authors wish to thank Christopher Gosdin (FPoliSolutions, LLC) for his valuable contribution to the preparation of the HATAC C2 input file for the TRANSURANUS code. The authors also thank Ville Peri from FORTUM (Finland), who implemented the original version of the ANS-5.4 model in the TRANSURANUS code. This project has received funding from the Euratom research and training programme 2014–2018 under grant agreement No 847656.

Appendix A. Effect of the coalescence model on fission gas release

The purpose of the present appendix is to show how the use of different grain-boundary bubble coalescence models, within the fission gas behaviour description, affects the predicted fission gas release. In Sec. 3, we applied the standalone version of TRANSURANUS (with the mechanistic setting for the fission gas behaviour) and the coupled-code version TRANSURANUS//SCIANTIX to compute the fission gas release during the CONTACT 1 experiment (Fig. 4), and the HATAC C2 experiment (Fig. 9). In both simulations, the fission gas release predicted by TRANSURANUS is lower than that predicted by TRANSURANUS//SCIANTIX. The role of the grain-boundary bubble evolution influences the predicted fission gas release, and in particular, the two codes adopt a mechanistic description for the grain-boundary bubble evolution that considers bubble growth and coalescence with different coalescence models.

The model describing the coalescence of grain-boundary bubbles, currently implemented in SCIANTIX, relies on the original work by White [55]. Namely, considering a spherical fuel grain uniformly covered with N (bub m^{-2}) identical bubbles per unit surface, and each bubble with an average (projected) area A (m^2), the rate of bubble loss due to coalescence following the area increase (i.e., the coalescence rate) is given by: $\frac{dN}{dA} = -2N^2$. The TRANSURANUS (mechanistic) option relies on the work of Pastore et al. [30,65], with a coalescence rate given by $\frac{dN}{dA} = -\frac{6N^2}{3+4NA}$. According to these formulations, the coalescence rate proposed by White implies a faster coalescence process. As a consequence, the use of the White coalescence model results in a higher fission gas release, with respect to the model of Pastore et al. [30].

To corroborate the discussion, we show radial profiles of the fission gas concentration, before and after the third power transient of the HATAC C2 test (where the re-irradiation history is shown in Fig. 8), at the mid-plane of the rodlet.

The radial profiles of the fission gas concentrations computed with TRANSURANUS are shown in Fig. 11a and b, before and after the power transient, respectively. Similarly, the radial profiles computed with TRANSURANUS//SCIANTIX are shown in Fig. 12a and b, before and after the power transient, respectively. The codes evaluate the concentration of fission gas produced (up to the beginning of the third power transient), intra-granular gas, gas accumulated at the grain boundaries, and gas released. Afterwards, we calculate the percentage variations in the radial concentration of intra-granular (Fig. 13a) and grain-boundary (Fig. 13b) fission gas, throughout the power transient. The variation is defined as positive for gas accumulation and negative for gas depletion.

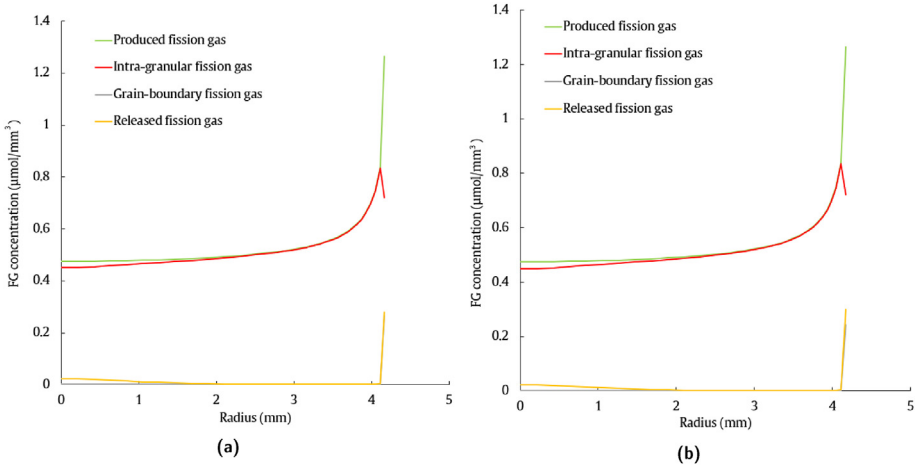

Fig. 11. Radial profiles of fission gas concentrations calculated with TRANSURANUS, before (a) and after (b) the third HATAC C2 power transient.

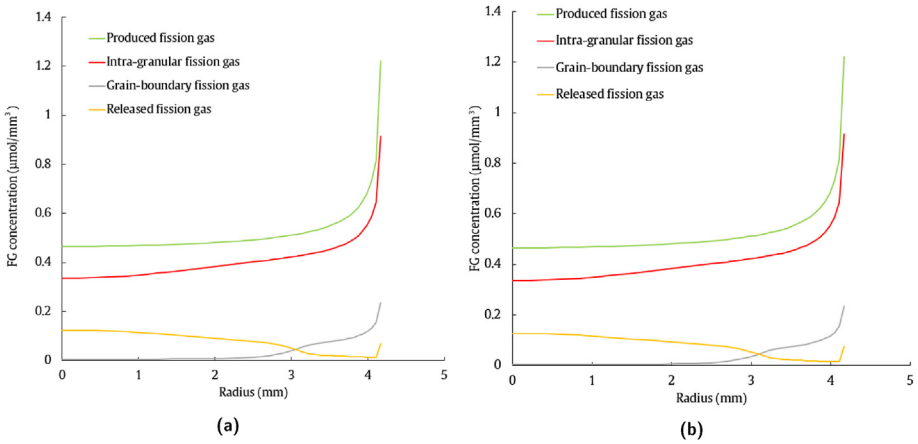

Fig. 12. Radial profiles of fission gas concentrations calculated with TRANSURANUS//SCIANTIX, before (a) and after (b) the third power transient.

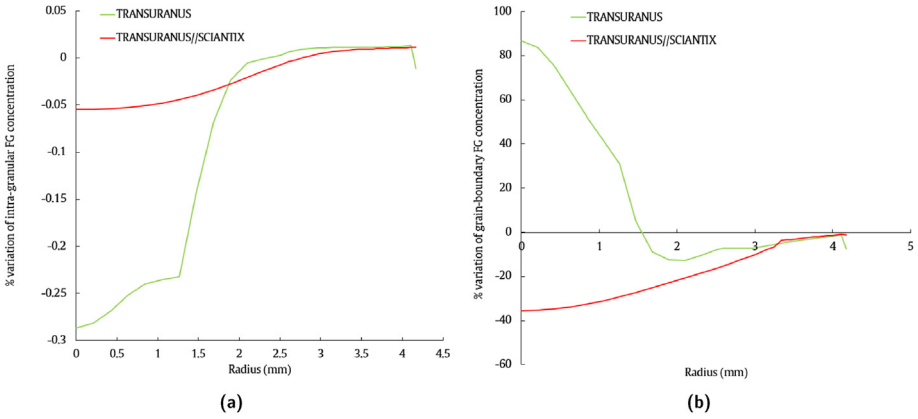

Fig. 13. Percentage variations of intra-granular (a) and grain-boundary (b) fission gas concentrations calculated with TRANSURANUS and TRANSURANUS//SCIANTIX, during the third HATAC C2 power transient.

The gas variation in the intra-granular region (Fig. 13a) shows that both the codes predict mostly an intra-granular gas depletion (due to gas diffusion). Namely, during the power transient, the gas diffuses from the intra-granular region towards the grain-boundary.[15] The gas variation in the grain-boundary region (Fig. 13b) shows that TRANSURANUS//SCIANTIX predicts a gas depletion across the entire radial dimension (resulting in increased gas release). In contrast, TRANSURANUS predicts a gas accumulation in the central part of the pellet and a small gas depletion in the peripheral part of the pellet. The sign of the gas variation (i.e., accumulation/release) is a consequence of the adopted bubble coalescence model, which determines the proportion of gas that can be released. Lastly, the gas variation within the grain-boundary region predominates over the intra-granular one, highlighting the impact of a different coalescence model.

References

[1] C. Wen, D. Yun, X. He, Y. Xin, W. Li, Z. Sun, Applying multi-scale simulations to materials research of nuclear fuels: a review, Mater. Rep.: Energy 1 (2021), 100048, https://doi.org/10.1016/J.MATRE.2021.100048.

[2] R. Martineau, D. Andrs, R. Carlsen, D. Gaston, J. Hansel, F. Kong, A. Lindsay, C. Permann, A. Slaughter, E. Merzari, R. Hu, A. Novak, R. Slaybaugh, Multiphysics for nuclear energy applications using a cohesive computational framework, Nucl. Eng. Des. 367 (2020), 110751, https://doi.org/10.1016/J.NUCENGDES.2020.110751.

[3] O.-N. NSC, State-of-the-art Report on Multi-Scale Modelling of Nuclear Fuels, Nuclear Science October.

[4] M.S. Veshchunov, A.V. Boldyrev, A.V. Kuznetsov, V.D. Ozrin, M.S. Seryi, V.E. Shestak, V.I. Tarasov, G.E. Norman, A.Y. Kuksin, V.V. Pisarev, D.E. Smirnova, S.V. Starikov, V.V. Stegailov, A.V. Yanilkin, Development of the advanced mechanistic fuel performance and safety code using the multi-scale approach, Nucl. Eng. Des. 295 (2015) 116–126, https://doi.org/10.1016/J.NUCENGDES.2015.09.035.

[5] L. Holt, U. Rohde, M. Seidl, A. Schubert, P.V. Uffelen, R. Macián-Juan, Development of a general coupling interface for the fuel performance code transuranus – tested with the reactor dynamics code dyn3d, Ann. Nucl. Energy 84 (2015) 73–85, https://doi.org/10.1016/J.ANUCENE.2014.10.040.

[6] M. García, R. Tuominen, A. Gommlich, D. Ferraro, V. Valtavirta, U. Imke, P.V. Uffelen, L. Mercatali, V. Sanchez-Espinoza, J. Leppänen, S. Kliem, A serpent2-subchanflow-transuranus coupling for pin-by-pin depletion calculations in light water reactors, Ann. Nucl. Energy 139 (2020), 107213, https://doi.org/10.1016/J.ANUCENE.2019.107213.

[7] H. Suikkanen, V. Rintala, A. Schubert, P.V. Uffelen, Development of coupled

[15] Differences in intra-granular gas variation are mainly attributable to the solution of the intra-granular diffusion equation, related to the FORMAS algorithm [66] in the TRANSURANUS code, while to the PolyPole algorithm [13,14] in the SCIANTIX code.

neutronics and fuel performance analysis capabilities between serpent and transuranus, Nucl. Eng. Des. 359 (2020), 110450, https://doi.org/10.1016/J.NUCENGDES.2019.110450.
[8] T.R. Pavlov, F. Kremer, R. Dubourg, A. Schubert, P.V. Uffelen, Towards a More Detailed Mesoscale Fission Product Analysis in Fuel Performance Codes: a Coupling of the Transuranus and Mfpr-F Codes, 2018.
[9] K. Lassmann, Transuranus: a fuel rod analysis code ready for use, Nuclear Mater. Fission React. (1992) 295–302, https://doi.org/10.1016/b978-0-444-89571-4.50046-3.
[10] A. Magni, A.D. Nevo, L. Luzzi, D. Rozzia, M. Adorni, A. Schubert, P.V. Uffelen, Chapter 8 - the Transuranus Fuel Performance Code, 2021, https://doi.org/10.1016/B978-0-12-818190-4.00008-5.
[11] D. Pizzocri, T. Barani, L. Luzzi, Sciantix: a new open source multi-scale code for fission gas behaviour modelling designed for nuclear fuel performance codes, J. Nucl. Mater. 532 (2020), 152042, https://doi.org/10.1016/j.jnucmat.2020.152042.
[12] T. Barani, D. Pizzocri, F. Cappia, L. Luzzi, G. Pastore, P. V. Uffelen, Modeling high burnup structure in oxide fuels for application to fuel performance codes. part i: high burnup structure formation, J. Nucl. Mater. 539. doi:10.1016/j.jnucmat.2020.152296.
[13] D. Pizzocri, C. Rabiti, L. Luzzi, T. Barani, P.V. Uffelen, G. Pastore, Polypole-1: an accurate numerical algorithm for intra-granular fission gas release, J. Nucl. Mater. 478 (2016) 333–342, https://doi.org/10.1016/j.jnucmat.2016.06.028.
[14] G. Pastore, D. Pizzocri, C. Rabiti, T. Barani, P.V. Uffelen, L. Luzzi, An effective numerical algorithm for intra-granular fission gas release during non-equilibrium trapping and resolution, J. Nucl. Mater. 509 (2018) 687–699, https://doi.org/10.1016/j.jnucmat.2018.07.030.
[15] G. Zullo, D. Pizzocri, L. Luzzi, On the use of spectral algorithms for the prediction of short-lived volatile fission product release: methodology for bounding numerical error, Nucl. Eng. Technol. 54 (2022) 1195–1205, https://doi.org/10.1016/J.NET.2021.10.028.
[16] W.L. Oberkampf, T.G. Trucano, C. Hirsch, Verification, validation, and predictive capability in computational engineering and physics, Appl. Mech. Rev. 57 (2002) 345–384, https://doi.org/10.1115/1.1767847.
[17] EERA-JPNM, Inspyre - Investigations Supporting Mox Fuel Licensing in Esnii Prototype Reactors, 2017.
[18] P. V. Uffelen, A. Schubert, L. Luzzi, T. Barani, A. Magni, D. Pizzocri, M. Lainet, V. Marelle, B. Michel, B. Boer, S. Lemehov, A. D. Nevo, Incorporation and verification of models and properties in fuel performance codes, INSPYRE Deliverable D7.2.
[19] L. Luzzi, T. Barani, B. Boer, L. Cognini, A.D. Nevo, M. Lainet, S. Lemehov, A. Magni, V. Marelle, B. Michel, D. Pizzocri, A. Schubert, P.V. Uffelen, M. Bertolus, Assessment of three european fuel performance codes against the superfact-1 fast reactor irradiation experiment, Nucl. Eng. Technol. 53 (2021) 3367–3378, https://doi.org/10.1016/j.net.2021.04.010.
[20] J. A. Turnbull, C. E. Beyer, Background and Derivation of ans-5.4 Standard Fission Product Release Modeldoi:10.2172/1033086.
[21] G. Zullo, D. Pizzocri, A. Magni, P. V. Uffelen, A. Schubert, L. Luzzi, Towards Grain-Scale Modelling of the Release of Radioactive Fission Gas from Oxide Fuel . Part I: Sciantix, Nuclear Engineering and Technologydoi:10.1016/J.NET.2022.02.011.
[22] M. Bruet, J. Dodelier, P. Melin, M.-L. Pointund, Contact 1 and 2 Experiments: Behaviour of Pwr Fuel Rod up to 15000 Mwd/tu, 1980, pp. 235–244.
[23] M. Charles, J.J. Abassin, D. Baron, M. Bruet, P. Melin, Utilization of Contact Experiments to Improve the Fission Gas Release Knowledge in Pwr Fuel Rods, 1983, pp. 1–18.
[24] D. Yun, J. Rest, G.L. Hofman, A.M. Yacout, An initial assessment of a mechanistic model, grass-sst, in u–pu–zr metallic alloy fuel fission-gas behavior simulations, J. Nucl. Mater. 435 (2013) 153–163, https://doi.org/10.1016/J.JNUCMAT.2012.12.024.
[25] J. Rest, A generalized model for radiation-induced amorphization and crystallization of u3si and u3si2 and recrystallization of uo2, J. Nucl. Mater. 240 (1997) 205–214, https://doi.org/10.1016/S0022-3115(96)00714-3.
[26] J. Rest, A model for the influence of microstructure, precipitate pinning and fission gas behavior on irradiation-induced recrystallization of nuclear fuels, J. Nucl. Mater. 326 (2004) 175–184, https://doi.org/10.1016/J.JNUCMAT.2004.01.009.
[27] R.J. White, M.O. Tucker, A new fission-gas release model, J. Nucl. Mater. 118 (1983) 1–38, https://doi.org/10.1016/0022-3115(83)90176-9.
[28] M.S. Veshchunov, V.I. Tarasov, Modelling of irradiated uo2 fuel behaviour under transient conditions, J. Nucl. Mater. 437 (2013) 250–260, https://doi.org/10.1016/J.JNUCMAT.2013.02.011.
[29] M.S. Veshchunov, V.D. Ozrin, V.E. Shestak, V.I. Tarasov, R. Dubourg, G. Nicaise, Development of the mechanistic code mfpr for modelling fission-product release from irradiated UO_2 fuel, Nucl. Eng. Des. 236 (2006) 179–200, https://doi.org/10.1016/j.nucengdes.2005.08.006.
[30] G. Pastore, L. Luzzi, V.D. Marcello, P.V. Uffelen, Physics-based modelling of fission gas swelling and release in UO_2 applied to integral fuel rod analysis, Nucl. Eng. Des. 256 (2013) 75–86, https://doi.org/10.1016/j.nucengdes.2012.12.002.
[31] M.R. Tonks, D. Andersson, S.R. Phillpot, Y. Zhang, R. Williamson, C.R. Stanek, B.P. Uberuaga, S.L. Hayes, Mechanistic materials modeling for nuclear fuel performance, Ann. Nucl. Energy 105 (2017) 11–24, https://doi.org/10.1016/J.ANUCENE.2017.03.005.
[32] R2ca (Reduction of Radiological Consequences of Design Basis and Extension Accidents, 2019.
[33] IAEA, Safety Reports Series No. 53, Derivation of the Source Term and Analysis of the Radiological Consequences for the Design Basis Accidents at Research Reactor, vol. 178, 2008, 978-992-0-109707-1.
[34] Safety of Nuclear Power Plants: Design, INTERNATIONAL ATOMIC ENERGY AGENCY, 2016.
[35] B. Dong, L. Li, C. Li, W. Zhou, J. Yin, D. Wang, Review on models to evaluate coolant activity under fuel defect condition in pwr, Ann. Nucl. Energy 124 (2019) 223–233, https://doi.org/10.1016/j.anucene.2018.10.009.
[36] B.J. Lewis, P.K. Chan, A. El-Jaby, F.C. Iglesias, A. Fitchett, Fission product release modelling for application of fuel-failure monitoring and detection - an overview, J. Nucl. Mater. 489 (2017) 64–83, https://doi.org/10.1016/j.jnucmat.2017.03.037.
[37] C. Vitanza, E. Kolstad, U. Graziani, Fission Gas Release from UO_2 Pellet Fuel at High Burn-Up, OECD HALDEN REACTOR PROJECT, 1979, pp. 361–366.
[38] M.S. Veshchunov, Mechanisms of fission gas release from defective fuel rods to water coolant during steady-state operation of nuclear power reactors, Nucl. Eng. Des. 343 (2019) 57–62, https://doi.org/10.1016/J.NUCENGDES.2018.12.021.
[39] H. Faure-Geors, D. Baron, C. Struzik, Hatac Experiments (1965-1990) Fission Gas Release at High Burn-Up, Effect of a Power Cycling, 1990.
[40] A. Magni, L. Luzzi, D. Pizzocri, A. Schubert, P.V. Uffelen, A.D. Nevo, Modelling of thermal conductivity and melting behaviour of minor actinide-mox fuels and assessment against experimental and molecular dynamics data, J. Nucl. Mater. 557 (2021), 153312, https://doi.org/10.1016/j.jnucmat.2021.153312.
[41] A. Cechet, S. Altieri, T. Barani, L. Cognini, S. Lorenzi, A. Magni, D. Pizzocri, L. Luzzi, A new burn-up module for application in fuel performance calculations targeting the helium production rate in (u,pu)o2 for fast reactors, Nucl. Eng. Technol. 53 (2021) 1893–1908, https://doi.org/10.1016/j.net.2020.12.001.
[42] D. Pizzocri, G. Pastore, T. Barani, A. Magni, L. Luzzi, P.V. Uffelen, S.A. Pitts, A. Alfonsi, J.D. Hales, A model describing intra-granular fission gas behaviour in oxide fuel for advanced engineering tools, J. Nucl. Mater. 502 (2018) 323–330, https://doi.org/10.1016/j.jnucmat.2018.02.024.
[43] T. Barani, G. Pastore, A. Magni, D. Pizzocri, P.V. Uffelen, L. Luzzi, Modeling intra-granular fission gas bubble evolution and coarsening in uranium dioxide during in-pile transients, J. Nucl. Mater. 538 (2020), 152195, https://doi.org/10.1016/j.jnucmat.2020.152195.
[44] L. Cognini, A. Cechet, T. Barani, D. Pizzocri, P.V. Uffelen, L. Luzzi, Towards a physics-based description of intra-granular helium behaviour in oxide fuel for application in fuel performance codes, Nucl. Eng. Technol. 53 (2021) 562–571, https://doi.org/10.1016/j.net.2020.07.009.
[45] R. Giorgi, A. Cechet, L. Cognini, A. Magni, D. Pizzocri, G. Zullo, A. Schubert, P.V. Uffelen, L. Luzzi, Physics-based modelling and validation of inter-granular helium behaviour in sciantix, Nucl. Eng. Technol. 54 (2022) 2367–2375, https://doi.org/10.1016/J.NET.2022.01.012.
[46] D. Pizzocri, F. Cappia, L. Luzzi, G. Pastore, V.V. Rondinella, P.V. Uffelen, A semi-empirical model for the formation and depletion of the high burnup structure in uo2, J. Nucl. Mater. 487 (2017) 23–29, https://doi.org/10.1016/j.jnucmat.2017.01.053.
[47] A. Magni, D. Pizzocri, L. Luzzi, M. Lainet, B. Michel, Application of the sciantix fission gas behaviour module to the integral pin performance in sodium fast reactor irradiation conditions, Nucl. Eng. Technol.doi:10.1016/J.NET.2022.02.003.
[48] T. Barani, E. Bruschi, D. Pizzocri, G. Pastore, P.V. Uffelen, R.L. Williamson, L. Luzzi, Analysis of transient fission gas behaviour in oxide fuel using bison and transuranus, J. Nucl. Mater. 486 (2017) 96–110, https://doi.org/10.1016/j.jnucmat.2016.10.051.
[49] Y. Perin, Development of a Multi-Physics, Multi-Scale Simulation Tool for Lwr Safety Analysis, vol. 9, 2016.
[50] S.J. Chapman, Fortran for Scientists and Engineers, McGraw-Hill Higher Education, NY, 2017.
[51] K. Lassmann, A. Schubert, P.V. Uffelen, C. Gyori, J. van de Laar, TRANSURANUS Handbook, Copyright © 1975-2014, 2014.
[52] (FUMAC), Fuel Modelling in Accident Conditions, IAEA, 2019, https://www.iaea.org/publications/13604/fuel-modelling-in-accident-conditions-fumac.
[53] The Research Reactor Siloe, Assoc. Belge Develop. Pacifique Energie At. Bull., Inform. Vol: vol. 8: No.
[54] G. Pastore, L.P. Swiler, J.D. Hales, S.R. Novascone, D.M. Perez, B.W. Spencer, L. Luzzi, P.V. Uffelen, R.L. Williamson, Uncertainty and sensitivity analysis of fission gas behavior in engineering-scale fuel modeling, J. Nucl. Mater. 456 (2015) 398–408, https://doi.org/10.1016/j.jnucmat.2014.09.077.
[55] R.J. White, The development of grain-face porosity in irradiated oxide fuel, J. Nucl. Mater. 325 (2004) 61–77, https://doi.org/10.1016/j.jnucmat.2003.10.008.
[56] A. Booth, A Method of Calculating Fission Gas Diffusion from UO_2 Fuel and its Application to the X-2-F Loop Test, Atomic Energy of Canada Limited.
[57] S. D. Beck, The Diffusion of Radioactive Fission Products from Porous Fuel Elements, Physics and Mathematics (TID-4500, fifteenth ed.).
[58] F.S. Ham, Theory of diffusion-limited precipitation, J. Phys. Chem. Solid. 6 (1958) 335–351, https://doi.org/10.1016/0022-3697(58)90053-2.
[59] M.V. Speight, A calculation on the migration of fission gas in material exhibiting precipitation and re-solution of gas atoms under irradiation, Nucl. Sci. Eng. 37 (1969) 180–185, https://doi.org/10.13182/nse69-a20676.
[60] M.S. Veshchunov, Modelling of grain face bubbles coalescence in irradiated

UO_2 fuel, J. Nucl. Mater. 374 (2008) 44–53, https://doi.org/10.1016/j.jnucmat.2007.06.021.
[61] N. Cayet (hwr–488), Investigation of Delayed Fission Gas Release, 1996.
[62] M.O. Tucker, J.A. Turnbull, The morphology of interlinked porosity in nuclear fuels, Proceed. Royal Soc. Lond. A. Math. and Phys. Sci. 343 (1975) 299–314, https://doi.org/10.1098/rspa.1975.0067.
[63] M.O. Tucker, The spacing of intergranular fission gas bubbles in irradiated uo\{2\}, J. Nucl. Mater. 74 (1978) 34–40.
[64] M.O. Tucker, A simple description of interconnected grain edge porosity, J. Nucl. Mater. 79 (1979) 199–205, https://doi.org/10.1016/0022-3115(79)90447-1.
[65] G. Pastore, Modelling of Fission Gas Swelling and Release in Oxide Nuclear Fuel and Application to the Transuranus Code, 2012, 1–110.
[66] K. Lassmann, H. Benk, Numerical algorithms for intragranular fission gas release, J. Nucl. Mater. 280 (2000) 127–135, https://doi.org/10.1016/S0022-3115(00)00044-1.